CORE SATURATION IN A MOVING MEDIUM

W. Kalkofen
Harvard-Smithsonian Center for Astrophysics, 60 Garden Street, Cambridge, MA 02138, U.S.A.

P. Ulmschneider
Institut für Theoretische Astrophysik, Im Neuenheimer Feld 294, 6900 Heidelberg, Federal Republic of Germany

ABSTRACT: We discuss a method of solving line transfer problems in moving media with plane symmetry. The method is an adaptation of the core saturation method of Rybicki (1972) to a medium with internal structure, such as shocks. Its speed follows from two simplifications: the neglect of detailed transfer in the line core, and the neglect of atmospheric regions that contribute negligibly to the formation of the emergent spectrum of interest.
In this version of core saturation, the separation of the line profile into core and wings is defined in terms of the monochromatic optical distance along rays between neighboring spatial grid points. In the line core, the specific, monochromatic intensity is assumed equal to the source function; in the wings, the intensity is obtained from a generalization of the Eddington-Barbier relation to an interior point of the medium, or from the first-order differential equation of transfer for the specific intensity, or from the formal integral assuming a piecewise linear source function.
The method has been tested with the calculation of a line source function in a static, isothermal medium and in a model solar atmosphere traversed by multiple shocks.

1. INTRODUCTION

In many time-dependent media of interest in astrophysics, energy is deposited by the dissipation of waves and is lost by radiation, often in only a small number of transitions. A typical case is a stellar chromosphere where the energy balance is believed to be between input from acoustic or magnetohydrodynamic waves (Ulmschneider & Stein 1982) and loss mainly in the strong resonance lines of Ca II, Mg II, and H I (Linsky 1980, 1981). In the quiet solar chromosphere (cf. Vernazza *et al.* 1981), 90% of the cooling occurs in these line transitions and less than 10% comes from H^- continuum radiation originating in the lowest and densest layers at the base of the chromosphere. Thus, if one wishes to model the time-dependent behavior of the middle chromosphere, for example, it is sufficient to treat the radiative loss in a few lines, or even in

a single, representative line.

For the numerical description of such a medium one needs a method for solving the transfer equation that is capable of giving a solution very fast since in a time-dependent problem, with typically 10^3 time steps, by far the largest fraction of the computer time tends to be used in the transfer calculation. Speed of the computation is therefore of the utmost importance. The description of some details of the transfer may have to be sacrificed; they can be calculated later from the known solution at particular time steps. Thus, it is important to treat macroscopic velocities that may be of the order of the sound velocity, but it will in general not be necessary - at least not for determining the overall structure of the medium - to treat partial redistribution with an anisotropic phase function. By restricting the transfer to complete frequency redistribution, and choosing a method that benefits from this simplification, one can gain perhaps two orders of magnitude in speed over the most general method, that of Grant, Hunt, and Peraiah (cf. Peraiah 1973, 1978). Further gains in speed are possible by confining the numerical treatment to those parts of the line profile where significant transfer occurs, namely the wings, and simplifying it in the line core, where radiation tends to be trapped and transfer takes place over regions where the properties of the medium change only little.

The critical feature of the transfer that permits a simple description of the radiation is that deep inside an atmosphere the mean intensity of radiation is equal to the source function, with corrections depending on the source function curvature and higher, even-order derivatives. This feature has been exploited by Kalkofen (1970) in approximating the discretized integral operator for the average intensity far from the boundaries of the medium by the identity matrix plus a tri-diagonal matrix representing the second derivative. Rybicki (1972) has used the relation between intensity and source function to build a numerical scheme for solving the transfer equation in statistical equilibrium, based on the simple physical idea of core saturation for sufficiently large monochromatic optical depth: in the line core, the monochromatic mean intensity is equal to the source function; in the wings it is determined from the transfer equation. Rybicki's method employed iteration in the wings and avoided the extensive storage requirements of other, more accurate methods.

Stenholm (1977) has extended Rybicki's core saturation approximation method to the solution of line transfer problems in media with geometries other than plane-parallel, and Scharmer (1981) has used it to derive a probabilistic equation similar to those of Athay (1972), Delache (1974), and Frisch & Frisch (1975).

The core saturation methods described above have in common that the separation of a line into core and wings is defined in terms of monochromatic optical distance of a point from the surface. They are thus unable to treat adequately media with internal structure, such as shocks. Since we wish to deal with such media we must allow for the exchange of energy between internal

points of the atmosphere. We therefore modify the definition of the line core in order to account for this energy transfer. In section 2 we state the basic equations of the transfer problem, define the separation of the line profile into core and wings, and describe several ways of calculating the specific intensity in the line wings; in section 3 we discuss numerical tests performed with an isothermal static atmosphere and with a moving medium representing a layer of the solar atmosphere; and in section 4 we summarize the results and present conclusions.

2. THE BASIC EQUATIONS

2.1 The Transfer Problem.

The transfer problem we wish to solve is defined by the line transfer equation and the equations of statistical equilibrium for the two combining states of the atom. We assume that the atmosphere has plane symmetry and that the kinetic temperature, T, the collision parameter, ϵ, and the velocity, q, of flow in the normal direction are known; for convenience we assume that they are given as functions of the optical depth, τ, at the undisplaced line center. For a line that is sufficiently strong that the background continuum may be ignored, the transfer equation may be written

$$\mu \frac{d}{d\tau} I(\tau, \nu, \mu) = \psi(\tau, \nu, \mu)(I(\tau, \nu, \mu) - S(\tau)) \quad , \tag{1}$$

where I is the specific, monochromatic intensity of the radiation field, μ the cosine of the angle between the direction of the photons and the outward normal, and ψ the absorption profile, given by the Voigt function,

$$\psi(\tau, \nu, \mu) = H(a, v) \quad , \tag{2}$$

(see Mihalas 1978 for references to tables of $H(a, v)$), where the parameter a is defined in terms of the damping constant Γ and the thermal Doppler width, $\Delta\nu_D$,

$$a(\tau) = \frac{\Gamma}{4\pi\Delta\nu_D} \quad , \tag{3}$$

and v is given by

$$v(\tau, \nu, \mu) = \frac{\nu - \nu_0 - (\nu_0/c)q\mu}{\Delta\nu_D} \quad . \tag{4}$$

For pure Doppler broadening, where $a = 0$, the function $\psi = 1$ at the displaced line center, $\nu = \nu_0(1 + (q/c)\mu)$; and in a static atmosphere, where $q = 0$, the reference optical depth coincides with the monochromatic optical depth at line center. The Voigt function ψ is related to the normalized profile function ϕ via

$$\phi(\tau, \nu, \mu) = \psi/(\sqrt{\pi}\Delta\nu_D) \quad , \tag{5}$$

whose frequence integral satisfies the condition

$$\int_0^\infty d\nu\phi(\tau,\nu,\mu) = 1 \quad . \tag{6}$$

The function S in the transfer equation (1) is the source function, which is assumed to be frequency-independent, corresponding to the assumption of complete redistribution of scattered photons. A formal expression for S is obtained from the equations of statistical equilibrium for the two combining states of the atom. If all transitions other than the direct radiative and collisional transitions are negligible, these equations can be cast into the form (cf. Thomas 1957, Jefferies 1968)

$$S = \frac{J+\epsilon B}{1+\epsilon} \quad , \tag{7}$$

where ϵ is the well-known collision parameter, B the Planck function, and J the integrated mean intensity,

$$J(\tau) = \frac{1}{2}\int_{-1}^{1} d\mu \int_0^\infty d\nu\phi(\tau,\nu,\mu)I(\tau,\nu,\mu) \quad . \tag{8}$$

The integral can be written as the sum of integrals over the line core and the line wings, defined below,

$$J(\tau) = \frac{1}{2}\int\limits_{\nu,\mu\in\, core} d\nu \int d\mu\,\phi I + \frac{1}{2}\int\limits_{\nu,\mu\in\, wings} d\nu \int d\mu\,\phi I \,, \tag{9}$$

which is a generalization of Rybicki's (1972) equation for the intensity in the core saturation method, where the separation into core and wings depends on frequency alone. The normalization integral may also be split into core and wing contributions, where the wing integral is defined as

$$\Omega(\tau) = \frac{1}{2}\int\limits_{\nu,\mu\in\, wings} d\nu \int d\mu\,\phi(\tau,\nu,\mu) \quad . \tag{10}$$

The equation suggests that we define a new profile function, $\chi_{\nu\mu} = \phi_{\nu\mu}/\Omega$, whose integral over wing frequencies and angles is normalized to unity (cf. Rybicki 1972). For the numerical work it is assumed that this normalization has been enforced.

The integral of the profile function over the line core may now be written

$$\frac{1}{2}\int\limits_{\nu,\mu\in\, core} d\nu \int d\mu\phi(\tau,\nu,\mu) = 1-\Omega(\tau) \quad . \tag{11}$$

Note that, in a static atmosphere, Ω is similar to an approximate, asymptotic expression for the escape probability from large depth (cf. Mihalas 1978, p. 341).

We now assume (cf. Rybicki 1972) that the value of the intensity in the line core is equal to the local value of the line source function,

$$I(\tau,\nu,\mu) = S(\tau)\,, \qquad \nu,\mu \in core \quad . \tag{12}$$

We thus neglect contributions made to the integral (9) over the intensity by the second and higher (even) derivatives of the source function. This is usually justified - even though the intensity is multiplied by the large core value of the profile function - since the second derivative is proportional to ϕ^{-2}; the exception is regions of very large source function gradients where the curvature of S might make a contribution. We may nevertheless make the assumption (12) since we could force the error to be arbitrarily small by choosing a criterion for the core-wing separation that treats most or all of the photons as wing photons, for which our integration solves the transfer equation without approximations, except those that are inherent in the discretization.

The core saturation approximation allows us now to write the equation (9) for the mean integrated intensity as

$$J(\tau) = S(1-\Omega)+\frac{1}{2}\int\limits_{\nu,\mu\in\, wings} d\nu \int d\mu\mu\phi I \quad , \tag{13}$$

and hence to simplify the source function equation to

$$S = \frac{\frac{1}{2}\int\limits_{\nu,\mu\in\, wings} d\nu \int d\mu\,\phi I + \epsilon B}{\Omega+\epsilon} \quad , \tag{14}$$

in which reference to core photons has been cancelled on both sides of the equation.

The specific, monochromatic intensity $I(\tau,\nu,\mu)$ at the depth τ depends on the emission $S(\tau)$ in a layer whose thickness is on the order of a photon mean-free-path, $\lambda_{\nu\mu}$. Thus equation (14) has the form of an integral equation,

$$S(\tau) = X(\tau,\tau')S(\tau')+Y(\tau) \quad , \tag{15}$$

with the angle and frequency integrated matrix operator X. If the equation is solved iteratively, for example by putting

$$S^{(n)}(\tau) = X(\tau,\tau')S^{(n-1)}(\tau')+Y(\tau) \quad . \tag{16}$$

where $S^{(n)}$ is the source function in the n^{th} approximation, it is impractical to avoid the approximation (12) to the transfer equation for core photons by extending the wings to the line center. The reason is the large number of iterations, of order $1/\epsilon$, that would be necessary to solve the resulting Neumann series (cf. Avrett & Hummer 1965). If the integral equation (15) is solved by inverting the matrix $(1-X)$, one can treat all photons as wing photons. But one loses the time-saving advantage of the core saturation method. It is then more efficient to include in equation (14) the second derivative term, which will play a role only in regions where the source function has significant curvature.

Another correction term in the source function equation can arise in a moving medium. The particle conservations equations will not simplify to the equations of statistical equilibrium if strong spatial gradients occur in the particle fluxes (cf. Kalkofen & Whitney 1971). The source function equation must then be corrected by a term that is proportional to the first derivative of the source function (cf. final chapter). This term can also easily be included in the matrix equation (15), but an iteration may still be necessary since that term can be non-linear.

It is interesting to note, as has been pointed out by Rybicki (1972), that the source function equation (14) gives directly an estimate of the thermalization distance, where $S \sim B$: If we assume that $I \sim S$ deep in the atmosphere, the wing integral is approximately equal to S. Now, Ω is essentially the escape probability, which for Doppler broadening, for example, is given by

$$\Omega \approx 1/\left(4\sqrt{\pi}\tau\sqrt{\ln\tau}\right)$$

(cf. the article by Canfield *et al.*, eq. 8.22). Hence, when the optical depth τ is of order $1/\epsilon$, the source function S is of the order of the Planck function B. Thus $1/\epsilon$ is an estimate of the thermalization length for a Doppler broadened line in a static atmosphere.

2.2 The Core - Wing Separation.

In the standard core saturation method as introduced by Rybicki (1972) and developed further by Stenholm (1977) and Scharmer (1981), the separation of line photons into core and wing photons is defined in terms of the optical depth of a given point. This procedure treats the escape of radiation from the surface of the medium but ignores transfer within the medium. Thus, in this form, the core saturation method cannot deal with structure within the atmosphere, such as shocks, that lead to transfer of radiant energy between internal points of the medium.

Since we want to treat radiative transfer inside the atmosphere, as occurs when the temperature or the flow velocity far from the surface vary, we need a definition of line wings that gives to internal points the same status as to boundary points. We therefore consider a photon at any depth τ_k to be in

the core or in a wing of the line if the monochromatic optical distance to the next grid point in the upstream direction for the photons under discussion is larger or smaller, respectively, than γ, a parameter of order unity, whose value depends on the requirements for computational speed and accuracy.

We use the usual convention in which the inward normal, $\mu = -1$, points along the positive τ-axis. The monochromatic optical distance, δ, for outward travelling photons between the spatial grid points τ_k and τ_{k+1} is then given by

$$\delta = \frac{1}{\mu_m}\overline{\psi} \times (\tau_{k+1} - \tau_k) \quad , \qquad \mu_m > 0 \quad , \tag{17}$$

where $\overline{\psi}$ is the average profile in the interval $(k, k+1)$,

$$\overline{\psi} = \frac{1}{2}[\psi(\tau_k, \nu_n, \mu_m) + \psi(\tau_{k+1}, \nu_n, \mu_m)] \tag{18}$$

for photons in the ray (ν_n, μ_m). The analogous definitions for inward travelling photons are

$$\delta = \frac{1}{\mu_m}\tilde{\psi} \times (\tau_k - \tau_{k-1}) \quad , \qquad \mu_m > 0 \quad , \tag{19}$$

for the optical distance between the grid points τ_k and τ_{k-1} along the ray $(-\nu_n, -\mu_m)$, with the average profile

$$\tilde{\psi} = \frac{1}{2}[\psi(\tau_k, \nu_n, \mu_m) + \psi(\tau_{k-1}, \nu_n, \mu_m)] \tag{20}$$

in the interval $(k, k-1)$.

Note that ν_n is the discretized frequence displacement, $\nu - \nu_o$, from the rest frequency, ν_o, of the line. The Voigt function (2), as well as the Doppler and Lorentz profiles, are symmetric about the displaced line center; hence (cf. Kalkofen 1970),

$$\phi(\tau, \nu_n, \mu_m) = \phi(\tau, -\nu_n, -\mu_m) \quad . \tag{21}$$

This property has been exploited here in the choices for the inward and outward rays and in writing the average profile (20). By combining the beams in this manner the numerical labor of computing optical depths is halved.

Now, if the optical distance from the spatial grid point k to the neighboring point $k+1$ is large, i.e.,

$$\delta > \gamma \quad , \tag{22}$$

the photons at the depth τ_k in the outward beam (ν_n, μ_m) are considered to be in the line core; similarly, if relation (22) is satisfied for the distance δ across the interval $(k, k-1)$, the corresponding photons in the inward beam $(-\nu_n, -\mu_m)$ belong to the core. The inequality (22) is not satisfied by photons in the four

line wings, which correspond to frequencies on either side of the line center, $\nu_n \gtrless 0$, and in the outward and inward beams, $\mu = \pm\mu_m$.

From the construction of the criterion (22) in terms of the optical distance across layers it is clear that if photons at the three-dimensional grid point (τ_k, ν_n, μ_m) are core photons, those at $(\tau_{k+1}, -\nu_n, -\mu_m)$ are also. This property can be exploited for reducing the work in a numerical solution.

For the treatment of shocks the criterion (22) is used in modified form: Recall that the typical spacing of depth points in an atmosphere is logarithmic. But when a shock is present, the distance between the shock point and a regular grid point can be very small. If the test (22) were applied to the optical distance between the shock point and this close grid point, there would be an influence on the computed intensity not only from the changed structure of the shocked medium but also from the change in the treatment of the core-wing separation. This is undesirable. In order to avoid favoring the shock point one wants to maintain the core-wing separation in the interval as though the additional shock point were not present. For the calculation of the intensity at the shock front we therefore scale the optical distance $\Delta\tau_s$ between the shock point and an adjacent grid point by the corresponding geometrical distance Δx_s and the geometrical thickness of the interval in which the shock is located, Δx. Thus (22) becomes $\Delta\tau_s \cdot \Delta x/\Delta x_s > \gamma$. Note that this procedure concerns only the definition of the line wings in an interval containing a shock point; the calculation of the intensity uses the appropriate optical distances.

2.3 The Intensity in the Line Wings.

For photons satisfying the inequality (22) the intensity is given by the assumption (12) of the saturated line core; for photons in a ray whose pathlength across the corresponding adjacent layer does not satisfy relation (22), the intensity is obtained from the transfer equation, either approximately or by means of an integration along the ray (ν_n, μ_m).

A simple approximation for the intensity is based on the assumptions that the source function depends linearly on monochromatic optical depth and that the distance to the boundaries is large. The specific intensity may then be determined from the values of the source function and its derivative. A convenient way of stating the relation between the source function and the specific intensity is to say that the intensity at τ_k is equal to the source function at unit optical distance from τ_k. Expressed in terms of the reference optical depth τ, this relation is

$$I(\tau_k, \nu, \mu) = S[\tau_k + \mu/\psi(\tau_k, \nu, \mu)] \quad . \tag{23}$$

This equation is the generalization of the well-known Eddington-Barbier relation (cf. Kourganoff 1963) for an interior point of the atmosphere.

Since the source points $\tau = \tau_k \pm \mu_m/\psi(\tau_k, \pm\nu_n, \pm\mu_m)$ do not, in general, coincide with any spatial grid point, it is necessary to interpolate the

value of the source function in equation (23). For this purpose we use the monochromatic optical depth, which is available from the test (22), and which yields a better interpolation value for the source point than the argument of the source function (23), for which the profile function at the depth τ_k was taken. With the notation δ_k^j for the optical distance along the rays (ν_n, μ_m) and $(-\nu_n, -\mu_m)$ between the spatial grid points τ_j and τ_k the interpolation formula is

$$I^+(\tau_k, \nu_n, \mu_m) = W S_j + (1-W) S_{j+1} \quad , \tag{24}$$

with

$$W = \left(\delta_k^{j+1} - 1\right)/\delta_j^{j+1} \quad , \tag{25}$$

where $(j, j+1)$ is the depth interval in which the source point for the outward intensity at τ_k is located; and for the inward intensity:

$$I^-(\tau_k, -\nu_n, -\mu_m) = W S_i + (1-W) S_{i-1} \quad , \tag{26}$$

with

$$W = (\delta_{i-1}^k - 1)/\delta_{i-1}^i \quad , \tag{27}$$

where $(i, i-1)$ is the depth interval containing the source point for I^-. The intervals $(j, j+1)$ and $(i, i-1)$ are to be chosen such that the source points are at unit optical distance along the corresponding rays from the field point τ_k at which the intensity is to be determined.

In regions of the atmosphere in which the source function depends linearly on depth, the Eddington-Barbier relation (23), or (24) to (27), gives the correct value for the intensity. In a time-dependent medium, however, the source function will rarely have this simple form. These expressions can then lead to a behavior that can be even qualitatively wrong. Near a saw tooth shock front, for example, the intensity from the Eddington-Barbier relation for the radiation on the low temperature side of the front, due to emission from the high temperature side, will exhibit an unphysical behavior as the point where it is computed approaches the front. The high emission from the hot side will have no effect on the intensity until the optical distance to the front is unity, when it will jump suddenly to a high value, and from then on the intensity will decrease with decreasing distance to the front since the single source point, where the emission is measured, moves to layers of lower temperature. The correct behavior of the intensity is a gradual increase with decreasing distance to the shock front, where the intensity reaches its maximal value. These difficulties can easily be avoided by a proper integration of the transfer equation; the simpler expression for the intensity should be used only when a sufficiently smooth depth dependence of the source function permits it.

For the calculation of the intensity in the line wings we may choose from several formulations. If we take the Feautrier equation, a second-order

finite difference equation, we obtain the intensity mean along a ray. Now, near a shock front, for example, the properties of the atmosphere change abruptly. Optical path lengths then change similarly, and a photon in the ray (ν_n, μ_m) might be a wing photon whereas a photon in the corresponding ray $(-\nu_n, -\mu_m)$ might be a core photon. With the Feautrier equation these photons would be treated jointly as though both were in the line wing. With the first-order equation (1), which yields the specific intensity, the core photon would be regarded as trapped and, hence, the core saturation approximation would be made, and the transfer equation would be solved only for the wing photon.

For short optical path lengths between neighboring grid points both equations give equally accurate results since the Feautrier equation has second-order accuracy and the first-order equation does so for half-implicit differencing. But for path lengths exceeding unity the first-order equation yields inferior results and for $\delta > 2$ the solution can become unstable unless the differencing is modified. The advantage of the first-order equation for our present purposes, however, is that it lends itself more readily to a formulation in which the transfer problem described by the integral equation (15) for the source function can be solved in one step by means of a matrix inversion; this is also true for the formal integral of the transfer equation.

We will give the weights for the integration of the first-order difference equation and for the discretized formal integral assuming piecewise linear segments of the source function (for the integration over quadratic segments, see Kalkofen 1974).

We write the transfer equation (1) in terms of the optical distance $\bar{\tau}$ along the rays (ν_n, μ_m) and $(-\nu_n, -\mu_m)$:

$$\bar{\tau}_k = \frac{1}{\mu} \int_0^{\tau_k} dt\, \psi(t, \nu_n, \mu_m) \quad . \tag{28}$$

At the spatial grid point τ_i the intensity I_i^+ in the outward ray (ν_n, μ_m) is obtained from the discretized transfer equation (1). Integrating along the ray across the layer $(i, i+1)$ we obtain

$$I_i^+ = a\, I_{i+1}^+ + b\, S_i + c\, S_{i+1} \quad , \tag{29}$$

where the coefficients a, b, and c depend on the optical path length across the layer $(i, i+1)$,

$$\delta = \bar{\tau}_{i+1} - \bar{\tau}_i \quad . \tag{30}$$

Similarly, for the inward intensity I_i^- along the ray $(-\nu_n, -\mu_m)$ we integrate across the layer $(i-1, i)$ to find

$$I_i^- = a\, I_{i-1}^- + b\, S_i + c\, S_{i-1} \quad , \tag{31}$$

with a, b, and c depending on δ:

$$\delta = \bar{\tau}_i - \bar{\tau}_{i-1} \quad . \tag{32}$$

Now, if the optical path δ is small, half-implicit differencing gives for the coefficients in the expressions (31) and (33) of the intensity:

$$a = \frac{2-\delta}{2+\delta}, \qquad b = c = \frac{\delta}{2+\delta}, \qquad \delta \leq 1 \, . \tag{33}$$

For a wider mesh we choose a differencing weight that guarantees a stable solution. The coefficients are then given by:

$$a = c = \frac{1}{2\delta+1}, \qquad b = \frac{2\delta-1}{2\delta+1}, \qquad \delta > 1 \, . \tag{34}$$

Note that the coefficients (33) for half-implicit differencing remain positive for $\delta < 2$. For the value $\delta = 1$ the integration constants (33) and (34) have the same value, ensuring a smooth transition between them.

The integration weights from the formal integral of the transfer equation are obtained from:

$$I_i^+ = \int_{\bar{\tau}_i}^{\bar{\tau}_{i+1}} dt\, e^{-(t-\bar{\tau}_i)}\, S(t) + I_{i+1}^+ \, e^{-(\bar{\tau}_{i+1}-\bar{\tau}_i)} \quad . \tag{35}$$

If we assume that the source function is a linear function of monochromatic optical depth in the layer $(i, i+1)$ we readily obtain an expression of the form (29) for the outward intensity where the coefficients are given by

$$a = e^{-\delta}, \qquad b = 1 - \frac{1-e^{-\delta}}{\delta}, \qquad c = e^{-\delta}\left(\frac{e^{\delta}-1}{\delta} - 1\right) \, , \tag{36}$$

in terms of the definition (30) for the path length δ. For short path length where rounding errors can affect the result we use instead the expansions

$$\begin{aligned} b &= \frac{\delta}{2}\left(1 - \frac{\delta}{3}\left(1 - \frac{\delta}{4}\cdots\right)\right) \, , \\ c &= e^{-\delta}\,\frac{\delta}{2}\left(1 + \frac{\delta}{3}\left(1 + \frac{\delta}{4}\cdots\right)\right) \, , \\ \delta &\ll 1 \quad . \end{aligned} \tag{37}$$

The expression for the inward intensity I_i^- from the formal integral has the same form as equation (31); the coefficients a, b, and c are also given by the

relations (36) or (37), in terms of the optical distance δ defined by equation (32).

The expressions (29) and (31) for the specific intensity I_k at the depth τ_k require the specification of boundary conditions. If these are chosen at an optical distance of at least $\delta\bar{\tau} = 5$ in the upstream direction, the emission further upstream contributes less than 1% - unless the source function increases sharply; then a larger value should be taken for $\delta\bar{\tau}$. At this "boundary" point, we set $I_j = S_j$, say, which is equivalent to assuming that the atmosphere is isothermal and semi-infinite beyond τ_j, with the intensity emerging at τ_j equal to S_j.

The above description of the integration of the transfer equation has considered the specific intensity only at the grid point τ_k. If the neighboring points in the downstream direction are closer than $\delta\bar{\tau} = \gamma$, the integration does not have to be started again sufficiently far upstream but needs to be carried only over the intervening layers.

2.4 The Net Radiative Cooling Rate.

With the specific intensity computed by means of equations (29) and (31), or the estimates (24) and (26), we can now determine the wing integral (13) of the intensity and hence the line source function by solving equation (15), either directly via a matrix inversion or iteratively according to the prescription (16). The knowledge of the line source function allows us then to calculate the local radiative cooling rate of the line without a further integration.

In order to define the cooling rate we write the transfer equation in terms of geometrical height as

$$\mu \frac{d}{dx} I = -\frac{h\nu_0}{4\pi} n_1 B_{12} \left(1 - \frac{n_2/\omega_2}{n_1/\omega_1}\right) \phi (I - S) \quad , \tag{38}$$

where the positive x-axis points along $\mu = 1, B_{12}$ is the Einstein coefficient for absorption in the transition from level 1 to level 2, and n and ω are the densities and weights of these levels. We wish to determine the flux, given by the intensity integral over solid angle and over the whole line profile,

$$F = \int d\Omega \int d\nu \mu I \quad . \tag{39}$$

The net radiative cooling rate, Φ, is then defined by the divergence of the radiative flux,

$$\frac{dF}{dx} = \Phi \quad , \tag{40}$$

and is given by

$$\Phi = h\nu_0 n_1 B_{12} \left(1 - \frac{n_2/\omega_2}{n_1/\omega_1}\right) (S - J) \quad . \tag{41}$$

We cast the expression into a more convenient form by eliminating reference to the population n_2 in the upper level with the aid of the source function, written in terms of the particle densities of the two combining states,

$$S = \frac{2h\nu_0^3}{c^2} \left(\frac{n_1/\omega_1}{n_2/\omega_2} - 1\right)^{-1} \quad , \tag{42}$$

and we eliminate reference to the mean integrated intensity with the help of the equation (7) of statistical equilibrium. We obtain

$$\Phi = h\nu_0 n_1 B_{12} \epsilon \frac{B - S}{1 + S/(2h\nu_0^3/c^2)} \quad . \tag{43}$$

Thus the local radiative cooling rate can be conveniently expressed in terms of the source function and the prescribed Planck function.

The solution method that we have described assumes that the structure of the underlying atmosphere is given in terms of the optical depth in the line. For the hydrodynamical calculations, however, the resulting cooling rate must be expressed in terms of geometrical or Lagrangian depth. The cooling rate must therefore be transformed into that space. If our procedure is to be useful, this transformation must not depend strongly on the source function. Fortunately this condition is often satisfied since the dominant radiative losses are typically due to radiative transfer in resonance lines of dominant ions. For weak sonic disturbances the ground state density is then insensitive to the solution for the source function so that our procedure can be used. Otherwise a further calculation is necessary to determine the transformation between the depth variables.

3. NUMERICAL TESTS

We have tested our method of solving the transfer problem with a static, isothermal medium and with a time-dependent model chromosphere traversed by multiple shocks using the quasi-static approximation for the equations of statistical equilibrium. Our aim was to study accuracy, convergence, and speed, and their dependence on the free parameter separating the line core from the wings.

The accuracy of the method is easiest to judge in a semi-finite, isothermal atmosphere with constant collision parameter and depth-independent, normalized absorption profile, where the surface value of the source function is given by $S(0) = \sqrt{\epsilon} B$, independent of the values of the Doppler and damping widths and of the number of angle points. Since the source function approaches the Planck function at large depth the error of the solution will tend to be maximal near the surface; we will characterize the accuracy of the method by the surface value.

3.1 The Isothermal Atmosphere.

We have solved the integral equation of the line transfer problem for the isothermal medium with $\epsilon = 0.01$ and a pure Doppler profile, using the iteration procedure indicated by equation (16). We discuss solutions with 34 depth points, covering the τ-range $0, 0.1, \ldots, 1000$, with one angle point, and with 21 frequency points in the half-profile.

The accuracy of the converged solution (cf. Table 1) depends mainly on the parameter γ (cf. eq. 22) defining the separation of core and wing frequencies in terms of the optical distance δ between adjacent grid points, and it depends only weakly on the method by which the intensity is calculated. Thus the source functions obtained by solving the transfer equation in differential equation form or from the formal integral have practically the same accuracy; for the solution employing the Eddington-Barbier relation it is lower.

The rate of convergence to the solution obtained after a very large number of iterations was independent of the method by which the transfer equation was integrated and depended on the wing parameter - the larger the value of γ, the more iterations were needed - and on the initial estimate of the source function, for which we took either $S(\tau) = B$ or $S(\tau) = \epsilon B$; the latter assumption saved two iterations. Table 2 lists the number of iterations required to reach the final solution to within a specified precision (in %), starting from $S = \epsilon B$ and setting $\gamma = 0.8$.

Table 1. Accuracy as a function of the monochromatic step length γ defining the separation of core and wing frequencies. The error, $(S(0)/0.1) - 1$, for the solution of the transfer equation with the differential equation (DE), the formal integral (IE), and the Eddington Barbier relation (EB).

γ	IE	DE	EB
0.8	2.0	2.5	3.6
1.0	-0.6	-0.2	
1.5	-2.8	-2.1	
2.0	-3.9	-3.4	

Table 2. Convergence rate for $\gamma = 0.8$: the number of iterations (IT) for reaching the converged solution to within a specified tolerance (E).

E	IT
10%	14
5%	17
2%	21
1%	24

The computing time necessary to determine the source function iteratively within 2% of the converged solution, which is comparable to the accuracy of the method for this value of γ, was longer than it would have taken solving the matrix equation directly. When the number of depth points was increased by 50%, the time per iteration increased linearly with the number of grid points, as did the number of iterations necessary to approach the final solution within specified bounds. Thus the increase in computing effort depended on the square of the number N of grid points. If we assume that this relation between accuracy and depth grid holds over a sufficiently wide range we may conclude that the iterative method of solution becomes comparable in efficiency with the solution by matrix inversion, which scales as N^3, when N is large enough. Since this value of N appears to be in excess of 10^2, the iterative solution would require less computing time only for grids as large as those often used in time-dependent hydrodynamical problems, but in the present problem the direct matrix inversion would have yielded the solution faster.

The calculation of the source function using the formal integral of the transfer equation takes 30% longer than using the differential equation. Since both solutions give nearly the same accuracy, the differential equation solution is preferable. The Eddington-Barbier solution of the transfer equation takes slightly less time but gives lower accuracy. Because of the expected difficulties near shock fronts (see also the discussion below) the time saved relative to the differential equation solution is not sufficient to compensate for its weaknesses except, perhaps, in problems with monotonic source function variation.

It is interesting that the differential and integral equations of transfer yield a source function solution of nearly the same accuracy. Since the monochromatic optical depth steps δ in the line wings are at most equal to γ one would expect higher, and different, accuracy from the two methods. A plausible explanation for the observed behavior would be that the error in the

source function is due mainly to the assumption of core saturation and that the integration of the transfer equation contributes only an insignificant error. This point is worth investigating further.

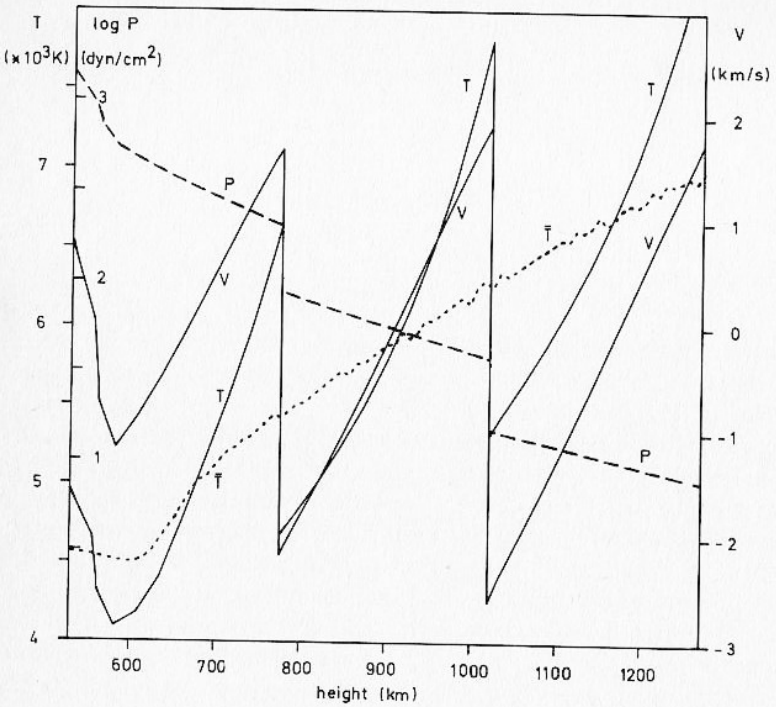

Fig. 1. Snapshot of the temperature, T, velocity, V, and pressure, P, as functions of height above $\tau_{5000} = 1$ for an acoustic wave in the solar chromosphere. The mean temperature, $\bar{T}$, time-averaged over a wave period is shown dotted.

3.2 The Moving Medium.

The aim of the calculation is to demonstrate the use of the method with the study of the formation of the k line of Mg II in the solar atmosphere. The model, shown in Figure 1, is a section of the solar chromosphere extending from the temperature minimum region to the middle chromosphere, taken at a particular time in the propagation of an acoustic wave (cf. Ulmschneider *et al.* 1978): v, p, and T are the instantaneous velocity, gas pressure, and kinetic temperature, respectively, and $\overline{T}$ is the time-averaged temperature, intended to match the temperature profile of static models of the quiet sun. This section of the atmosphere covers the optical depth range at the undisplaced line center from $\tau_0 = 3.5 \times 10^2$ at the top of the atmosphere to 7.0×10^5 at the lower boundary.

The parameters describing the Mg ion are: the abundance, $A = 3.9 \times 10^{-5}$; the rate coefficient for superelastic collisions, $\Omega_{21} = 3.6 \times 10^{-7}$; the radiative damping width, $\Gamma_{rad} = A_{21} = 2.7 \times 10^8$; and the elastic collision width,

$$\Gamma_e = 1.0 \times 10^{-8}(T/5000)^{0.3}\, n_H \quad ,$$

where the hydrogen density, n_H, is obtained from the mass density, ρ, of the model,

$$n_H = \rho/(1.4 m_H) \quad ,$$

with m_H the mass of the hydrogen atom. Electrons are assumed to be contributed by singly ionized metals, giving the fixed proportion for the electron density of $n_e = 10^{-4} \times n_H$.

In the atmosphere the collision parameter ϵ varies from 8.4×10^{-7} at the upper boundary to 2.6×10^{-4} at the lower, and the damping parameter in the Voigt profile, $a = (\Gamma_E + \Gamma_{Rad})/4\pi\Delta\nu_o$, is approximately equal to 3×10^{-3}. The velocity amplitude of the wave implies a frequency shift of about one thermal Doppler width.

The frequency grid consisted of 28 points distributed logarithmically and symmetrically about $|\Delta\lambda| = 0.036\mathring{A}$, corresponding to two thermal Doppler widths ($\sim 2\Delta\lambda_D$) on either side of the line center, out to $|\Delta\lambda| = 0.50\mathring{A}(\sim 27\Delta\lambda_D)$. At the outermost frequency points there was a contribution to the line wings even at the bottom boundary. The angle grid consisted of either one or three division points, which were chosen according to the requirements of Gaussian quadrature.

3.3 Comparison with the Standard Core Saturation Method.

For the static, time-averaged atmosphere ($v = 0, \bar{T}$) we have compared our version of core saturation, where the separation of the line profile into core and wings is defined in terms of the monochromatic optical distance along a ray between adjacent grid points, with the standard core saturation method (Rybicki 1972, Stenholm 1977, Scharmer 1981), where wing frequencies are defined in terms of monochromatic optical depth, i.e., normal ($\mu = 1$) optical distance to the surface. Figure 2 shows the core-wing diagram for the value $\gamma = 0.7$ of our parameter for the core-wing separation, and for $\tau_\gamma = 1.0$ and 2.7, typical values for the parameter in the standard method (Stenholm, private communication). The figure shows that the boundaries of the core for $\gamma = 0.7$ coincide with those for $\tau_\gamma = 2.7$ in the interior of the slab and for $\tau_\gamma = 1.0$ near the upper boundary. The source function for the time-averaged, static atmosphere is shown in Figure 3. The calculation is carried out for $\gamma = 0.7$ and with the initial estimates for the source function of $S = B$ and $S = \epsilon B$. As before, convergence to within 10% of the final solution occurs in about 14 iterations.

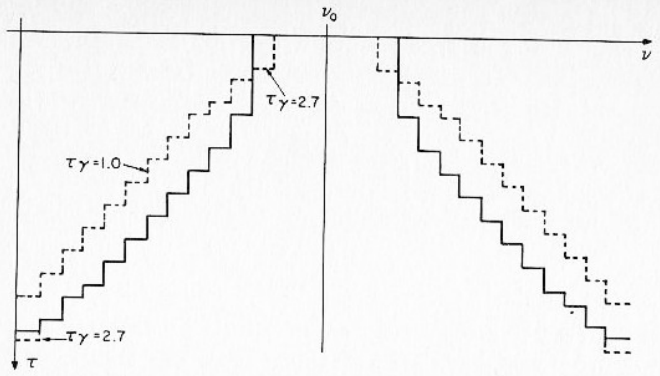

Fig. 2. Core-wing diagram for the mean atmosphere of Figure 1 with one angle point, 28 frequency points, and $\gamma = 0.7$. The core-wing diagrams of the standard core-saturation method for $\tau_\gamma = 1.0$ and 2.7 are shown dashed.

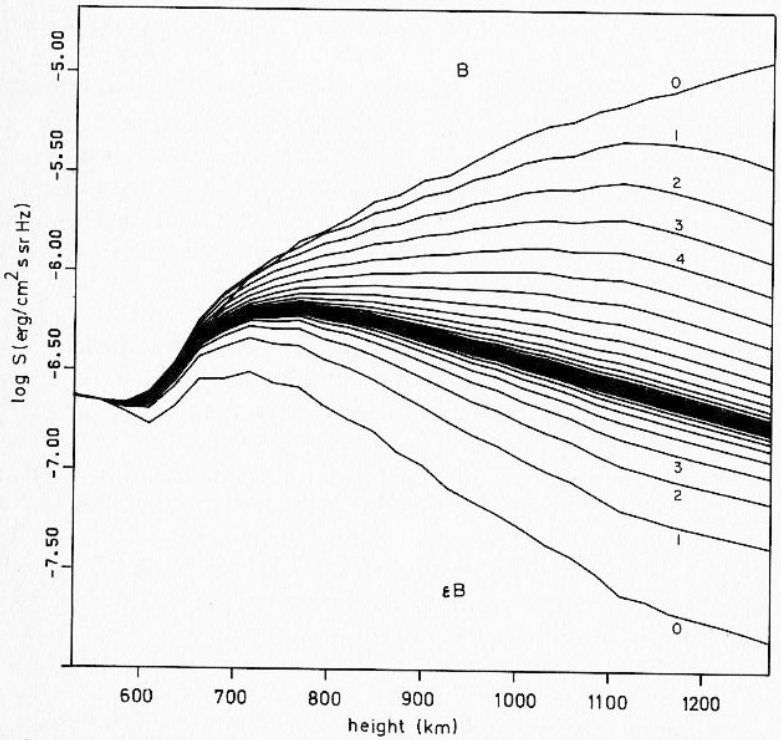

Fig. 3. Iteration of the source function S for the mean atmosphere with one angle, 28 frequency points, and $\gamma = 0.7$. Iteration numbers are indicated.

3.4 Variation of Angle and Frequency Grids.

For the moving atmosphere depicted in Figure 1 the temperature and velocity variations of the gas lead to an asymmetric core-wing diagram, shown in Figure 4 for the outward radiation at one angle point; the map for the inward radiation is essentially the mirror image. Note that the line center (ν_0) does not contribute wing photons even at the top of the atmosphere since the upper boundary is at the relatively large optical depth of 350. Note also that there are wing parts at intermediate depths that receive radiation from deeper and from shallower layers but do not lose radiation to the surface. The standard core saturation method would have treated them as core points, in which the intensity is equal to the source function, and thus would have failed to account properly for their energy exchange with the surrounding medium.

The source function for the moving atmosphere is shown in Figure 5, with the iterations starting again from $S = B$ or $S = \epsilon B$. As before, convergence (cf. Table 3) is faster with the initial solution $S = \epsilon B$; and the converged solution is reached earlier than in the isothermal atmosphere.

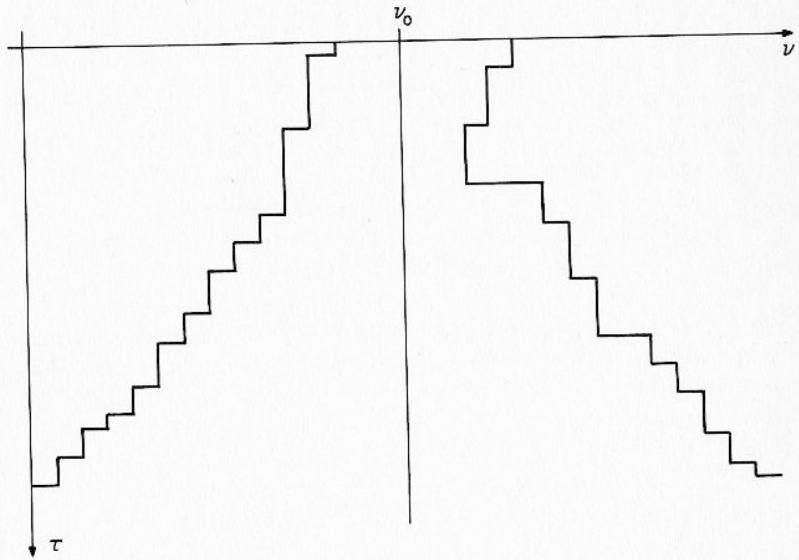

Fig. 4. Core-wing diagram for the actual atmosphere of Figure 1 and outgoing radiation with one angle point, 29 frequency points, and $\gamma = 0.7$.

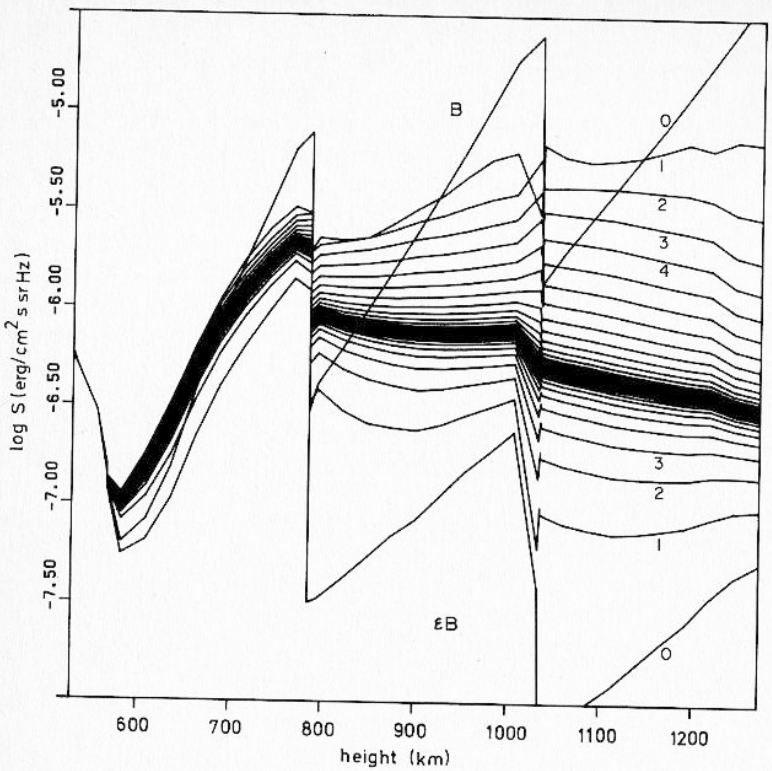

Fig. 5. Iteration of the source function S as function of height starting from $S = B$ (top) and from $S = \epsilon B$ (bottom) for the actual atmosphere of Figure 1 with one angle, 28 frequency points and $\gamma = 0.7$. Iteration numbers are indicated.

Table 3. Convergence rate in the moving atmosphere: number of iterations needed to reach the converged solution within specified tolerance.

	S = B		S = εB	
γ	10%	1%	10%	1%
0.5	12	17	8	14
0.7	14	20	8	16
1.0	16	24	11	19

As pointed out above, the assumption of core saturation is of no consequence for the solution when the source function depends linearly on monochromatic optical depth; but in regions where the source function depends on higher powers of τ the neglect of the curvature term degrades the solution. This can be seen in the results for increasing values of the parameter γ, with which the wings of the line, where the transfer equation is solved in detail, can be moved further towards the line center. Figure 6 shows the core-wing diagram for $\gamma = 0.5$, 0.7, and 1.0; the larger γ, the narrower is the line core; and the smaller is the error from the neglect of transfer in the core. The solutions for the source function with the three values of γ are given in Figure 7. The difference in the source functions for $\gamma = 0.7$ and 1.0 is quite small, except at the temperature minimum and, to a lesser extent, at the shock fronts, where the error from the neglect of the curvature term is noticeable. For the study of the energy loss from the solar chromosphere these errors are not serious since the cooling of the temperature minimum region is dominated by emission of H^-. In general, the remedy for low accuracy is a larger value of the core-wing separation parameter γ, or a narrower spacing of depth points in critical areas, which also has the effect of narrowing the line core.

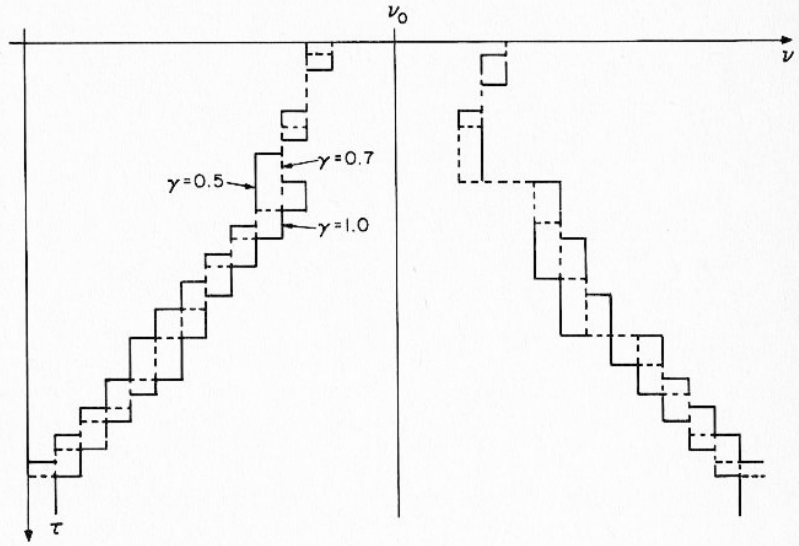

Fig. 6. Core-wing diagram as in Figure 4, but for $\gamma = 0.5$, 0.7, and 1.0.

The accuracy of the calculation improves also when the number of angle points in the moving medium is increased. Figure 8 shows the core-wing diagram for three angle points: The velocity effects are the most pronounced for the largest value of μ, since the projected velocity is proportional to μ, and the core is the widest for the smallest value of μ, since the optical path length is proportional to $1/\mu$. Figure 9 shows the source function for 28 frequency points with one or three angles, and for 56 frequencies with three angles. The solution for one angle point differs by about 5% from the two solutions with three angle points, which practically coincide. Thus, the smaller number of frequency points is sufficient for treating this problem; but in the angle discretization, three points per hemisphere are required if the accuracy is to be better than that of the core saturation approximation. At two angles, the errors are comparable, and taking more than three is unnecessary here since the velocity dependence of the profile in the damping wings, where almost all the frequency points are located, is quite small, so that over a large part of the frequency range the transfer is hardly different from that in a static atmosphere, where an increase in the number of angle points beyond three changes the solution by an insignificant amount.

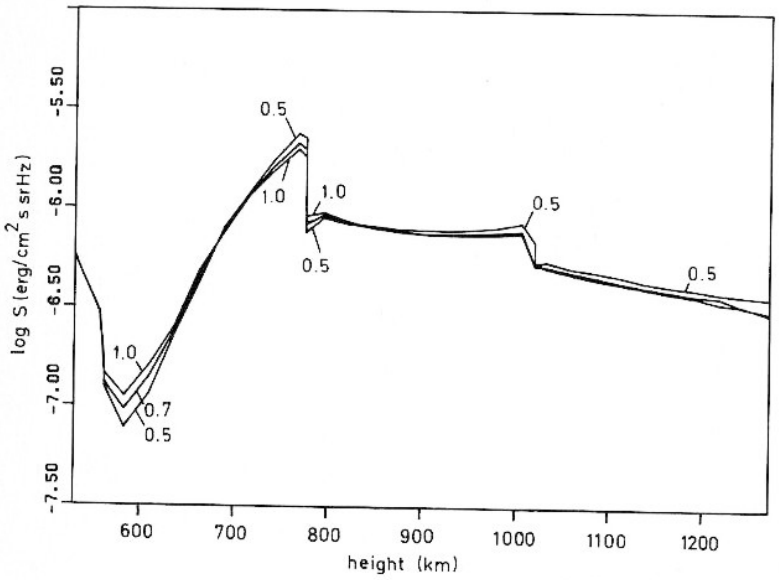

Fig. 7. Converged source functions for $\gamma = 0.5$, 0.7, and 1.0.

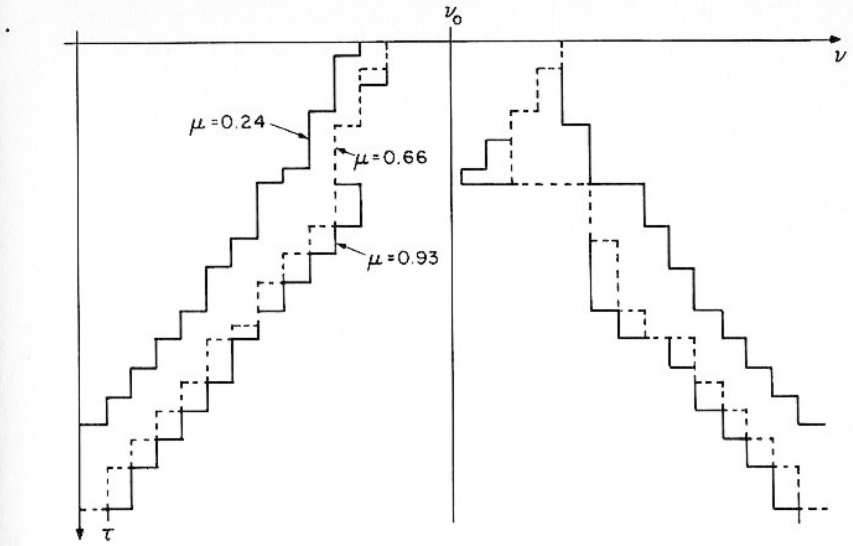

Fig. 8. Core-wing diagrams as in Figure 4, but for three angle points.

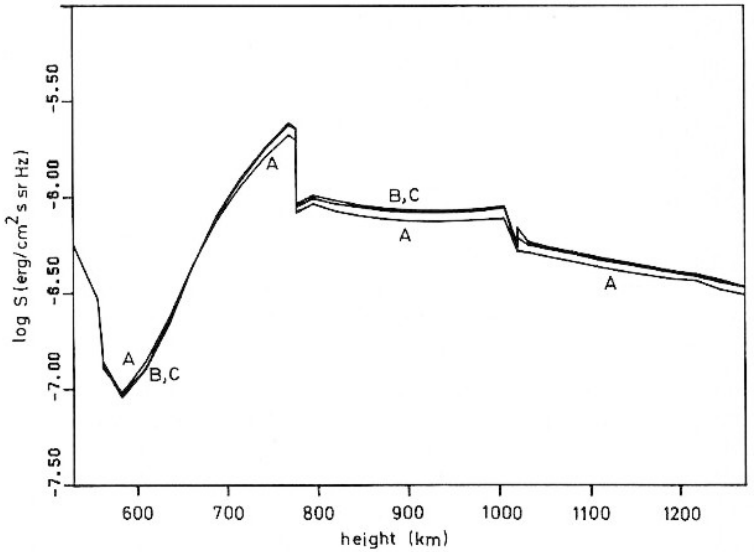

Fig. 9. Converged source functions for $\gamma = 0.7$ and for cases A: 1 angle, 28 frequency points, B: 3 angle, 28 frequency points and C: 3 angle, 56 frequency points.

The source function in the moving atmosphere was calculated by solving the transfer equation as a first-order finite-difference equation or by evaluating the Eddington-Barbier relation. The latter method has a considerable intrinsic advantage in speed, but the overall calculation gained only about 9% in time. This must be weighed against an increase in the error, which amounts to about 10% at the temperature minimum (cf. Figure 10), and a reduction of the source function on both sides of the shock fronts, which implies an increase in the computed net cooling rate (43) of the gas near the shocks. Thus, while the error of the Eddington-Barbier relation may, perhaps, be tolerable for source function calculations in which the temperature structure of the atmosphere is monotonic and is prescribed, in calculations in which that structure is to be determined it is much safer and not much more costly to solve the transfer equation in the differential or integral equation form.

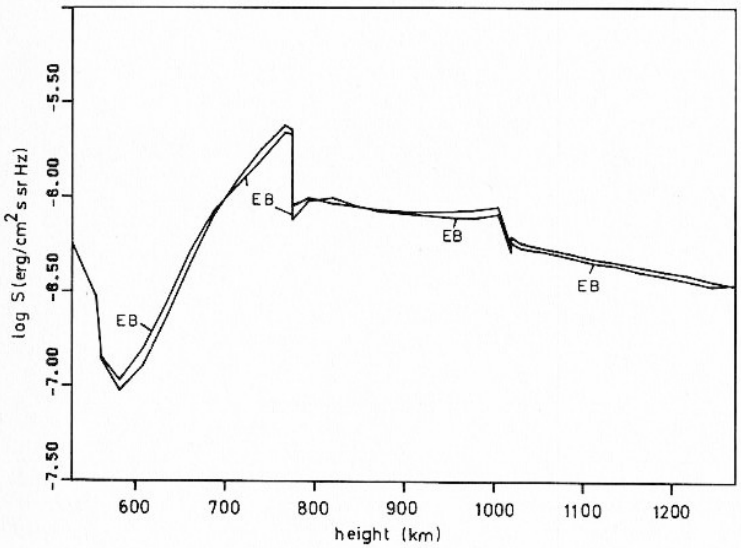

Fig. 10. Converged source functions for 3 angle, 28 frequency points and $\gamma = 0.7$. The solution labelled EB uses the Eddington-Barbier approximation for the specific intensity.

4. CONCLUSIONS

We have described a numerical method for solving the line transfer equation of a two-level atom in statistical equilibrium, assuming complete redistribution of emitted photons. The essence of the method is the assumption of saturation in the line core, which is defined, locally, by the requirement that the specific, monochromatic optical distance along a ray to the next spatial grid point in the upstream direction be larger than some value of order unity. If the condition is met, the specific, monochromatic intensity is set equal to the source function; otherwise the intensity is calculated from the generalization of the Eddington-Barbier relation, or from the first-order differential equation (ODE) for the specific intensity, or from the integral equation of transfer (formal integral), assuming piecewise linear segments of the source function.

We have studied speed and accuracy of the integration of the line transfer equation in a semi-infinite atmosphere with constant Planck function and constant collision parameter ϵ, and of a Mg II resonance line in a model solar atmosphere traversed by shocks. In the latter problem, the upper boundary was at the relatively large line depth of $\tau_0 = 3.5 \times 10^2$. The reason for the neglect of the top layer of the atmosphere was that we were interested only in the intensity in the line wings. The justification for the neglect is that the top layer contributes negligibly to the wing intensity. The numerical work is thereby reduced.

We have solved the matrix equation of the problem, which has the same structure as the equation in the integral equation method, by means of an iteration scheme. The calculation would have been faster with the direct solution of the system of linear equations for the source function values. A considerable further speed-up, useful for time-dependent problems, would have resulted with a perturbation of the integral operator, as proposed by Cannon (this volume) and implemented by Scharmer (this volume) (see also concluding chapter).

For a medium with arbitrary temperature and velocity structure, the best results were obtained with the calculation of the specific intensity from the transfer equation as a first-order ODE.

5. ACKNOWLEDGEMENTS:

This work has been supported in part by the NASA grant NAGW-253, by the Deutsche Forschungsgemeinschaft (SFB132), and by the Secretary's Fluid Research Fund of the Smithsonian Institution.

6. REFERENCES

Athay, R. G. 1972. *Astrophys. J.*, **176**, 659.
Avrett, E. H., & Hummer, D. G. 1965. *Mon. Not. R. Astr. Soc.*, **130**, 295.
Canfield, R. C., McClymont, A. N., & Puetter, R. C., this volume.
Delache, P. 1974. *Astrophys. J.*, **192**, 475.
Frisch, U., & Frisch, H. 1975. *Mon. Not. R. Astr. Soc.*, **173**, 167.
Jefferies, J. T. 1968. *Spectral Line Formation*. Blaisdell Publ. Co., Waltham, MA.
Kalkofen, W. 1970. In *Spectrum Formation in Stars with Steady-State Extended Atmospheres*, NBS Spec. Pub., **332**, 120.
_ . 1974. *Astrophys. J.*, **188**, 105.
Kalkofen, W., & Whitney, C. A. 1971. *J.Q.S.R.T.*, **11**, 531.
Kourganoff, V. 1963. *Basic Methods in Transfer Problems*, Dover, New York.
Linsky, J. L. 1980. *Ann. Rev. Astron. Astrophys.*, **18**, 439.
_ . 1981. In *Solar Phenomena in Stars and Stellar Systems*, ed. Bonnet, R. M. and Dupree, A. K., Reidel, Dordrecht.
Mihalas, D. 1978. *Stellar Atmospheres*, Freeman, San Francisco.
Peraiah, A. 1973. *J. Inst. Maths. Applics.*, **12**, 75.
_ . 1978. *Kodaikonal Obs. Bull., Ser. A*, **2**, 115.
Rybicki, G. B. 1972. In *Line Formation in Magnetic Fields*, NCAR, Boulder, CO, p. 145.
Scharmer, G. B. 1981. *Astrophys. J.*, **249**, 720.
Stenholm, L. G. 1977. *Astron. Astrophys.*, **54**, 577.
Thomas, R. N. 1957. *Astrophys. J.*, **125**, 260.
Ulmschneider, P., Schmitz., F., Kalkofen, W., & Bohn, H. U. 1978. *Astron. Astrophys.*, **70**, 487.
Ulmschneider, P., & Stein, R. F. 1982. *Astron. Astrophys.*, **106**, 9.
Vernazza, J. E., Avrett, E. H., & Loeser, R. 1981. *Astrophys. J. Suppl.*, **45**, 635.

NON-LOCAL PERTURBATION TECHNIQUES IN RADIATIVE TRANSFER

C.J. Cannon
Department of Applied Mathematics, The University of Sydney, N.S.W. 2006, Australia

The equation of radiative transfer reflects the direct coupling between the photon distribution at one point in the radiating gas and the photon distributions at all other points within a distance less than approximately a thermalisation path length. Any attempt at the numerical solution of the transfer equation must therefore adequately represent this non-local coupling, and this generally implies that a sufficient number of frequency, angle and position grid points must be chosen if the radiation field is to be satisfactorily described. More particularly, the precise manner in which photons interact with the atoms and ions constituting the plasma is contained in the redistribution function, and this can exhibit sharply peaked components in both frequency and angle space thus again necessitating care in constructing an appropriate frequency and angle grid network. These are important considerations not just from the mathematical desire to compute an accurate solution to the transfer equation, but from the more general point of view for which the transfer equation must, in turn, be coupled to the gas-dynamic conservation equations specifying the macroscopic quantities velocity, density and temperature. An inadequate numerical representation of the angle, frequency and position variables will lead to an inadequate representation of the radiation field. This will generate errors in the above velocities, densities and temperatures (these errors, of course, will feed back onto the solution of the transfer equation) and subsequently affect our understanding of the energy balance within the radiating gas.

All of the above discussion suggests that the number of required grid points needed to solve the transfer equation could be prohibitively large even when using very large computers. The thrust behind the perturbation technique is to remove this difficulty by solving a simpler reduced problem for which a smaller number of grid points, along with the more manageable complete redistribution assumption, is